

The potential role of atrial natriuretic peptide in the effects of Angiotensin-(1-7) in a chronic atrial tachycardia canine model

Journal of the Renin-Angiotensin-Aldosterone System
January-March 2016: 1-12
© The Author(s) 2016
Reprints and permissions:
sagepub.co.uk/journalsPermissions.nav
DOI: 10.1177/1470320315627409
jra.sagepub.com


Jun Zhao, Tiecheng Liu, Enzhao Liu, Guangping Li, Lingshan Qi and Jian Li

Abstract

Objective: The objective of this article is to investigate the possible role of atrial natriuretic peptide (ANP) in Angiotensin-(1-7) (Ang-(1-7)) signaling pathway on atrial electrical and structural remodeling in a chronic rapid atrial pacing canine model.

Methods: Twenty-four dogs were randomly assigned to four groups: a sham group, paced control group, a paced + Ang-(1-7) group and a paced + Ang-(1-7) + A-71915 group. Atrial rapid pacing (ARP) at 600 bpm was maintained for 14 days except in the animals from the sham group. During the pacing, Ang-(1-7) ($6 \mu\text{g}\cdot\text{kg}^{-1}\cdot\text{h}^{-1}$) or Ang-(1-7) ($6 \mu\text{g}\cdot\text{kg}^{-1}\cdot\text{h}^{-1}$) + A-71915 (ANP receptor antagonist, $0.30 \mu\text{g}\cdot\text{kg}^{-1}\cdot\text{h}^{-1}$) were given intravenously, respectively. After pacing, it was measured that electrophysiological parameters including atrial effective refractory periods (ERPs), inducibility and duration of atrial fibrillation (AF), I_{CaL} and I_{Na} changed, where I_{CaL} refers to voltage-dependent L-type Ca^{2+} current and I_{Na} refers to cardiac sodium current. Then, the fibrosis and the expression of Cav1.2, $I_{\text{Nav}}1.5\alpha$ subunit, TGF- β_1 and ANP in atria were assessed.

Results: After ARP, compared with the sham group, the atrial ERPs at six sites in each dog were shortened with the increasing in inducibility and duration of AF in the paced control group. The density of I_{CaL} , I_{Na} and the expression of Cav1.2, $I_{\text{Nav}}1.5\alpha$ subunit mRNA were decreased. Atrial tissue from the paced dogs showed significant interstitial fibrosis. The expression of TGF- β_1 and ANP in mRNA and protein levels were increased. Compared with the paced control group, the shortening of atrial ERPs, and the increasing of inducibility and duration of AF induced by ARP were alleviated by Ang-(1-7) treatment ($p < 0.05$). The density of I_{CaL} and I_{Na} and the expression of Cav1.2 and $I_{\text{Nav}}1.5\alpha$ subunit mRNA were slightly decreased. Atrial tissue showed less interstitial fibrosis after Ang-(1-7) treatment. The increasing of ANP expression was improved by Ang-(1-7), while the increasing of TGF- β_1 expression was alleviated by Ang-(1-7) ($p < 0.05$). A-71915 treatment blocked the beneficial effects of Ang-(1-7) on the aforementioned electrophysiological parameters and atrial fibrosis. And A-71915 treatment blocked Ang-(1-7), improving the expression of TGF- β_1 .

Conclusion: Ang-(1-7) prevented atrial structural and electrical remodeling induced by ARP. Furthermore, Ang-(1-7) promoted ANP secretion, and ANP played a crucial role in the cardiac protection of the former.

Keywords

Atrial fibrillation, rapid atrial pacing, Ang-(1-7), atrial natriuretic peptide

Date received: 27 September 2015; accepted: 22 December 2015

Introduction

The renin-angiotensin system (RAS) has been believed to participate in many cardiovascular diseases, especially in atrial tachycardia or atrial fibrillation (AF).¹ As it is known to us, Angiotensin II (Ang II) was the first member of the RAS confirmed to raise the risk of cardiac arrhythmia and relate to the progression of AF.^{2,3} Ang II has been carefully studied, till the innovative study from Schiavone and colleagues⁴ confirmed Ang-(1-7) was able to counterbalance

Tianjin Key Laboratory of Ionic-Molecular Function of Cardiovascular Disease, Department of Cardiology, Tianjin Institute of Cardiology, Second Hospital of Tianjin Medical University, People's Republic of China

Corresponding author:

Enzhao Liu, Tianjin Key Laboratory of Ionic-Molecular Function of Cardiovascular disease, Department of Cardiology, Tianjin Institute of Cardiology, Second Hospital of Tianjin Medical University, Tianjin 300211, People's Republic of China.
Email: liu_ezh@126.com



Ang II as a new member of the RAS.^{5,6} Recently, research has clarified the essential metabolic pathway of Ang-(1–7). It was converted by Ang II or neutral endopeptidase mainly from Angiotensin I (Ang I).⁷ As an alternative origin, Ang-(1–7) can be transformed directly from Ang II by the Ang-converting enzyme (ACE) 2, which is a homolog of ACE.⁸ In a recent study, Ang-(1–7) was implicated to decrease cardiac fibrosis through the Mas/PI3K/Akt/NO axis, which was participated in by the increased atrial natriuretic peptide (ANP) secretion *in vitro*.⁹ In our previous research, Ang-(1–7) proved able to prevent the shortening of atrial effective refractory periods (ERPs) and the increasing of AF vulnerability mediated by the Mas/PI3K/Akt/NO signaling pathway, in which ANP played a crucial role.¹⁰ Thus, the purpose of our present study was to investigate the potential role of ANP in the effects of Ang-(1–7) on chronic atrial remodeling in an atrial rapid pacing (ARP) canine model.

Methods and materials

Preparation of the canine model

We obtained experimental animal use approval from the Experimental Animal Administration Committee of Tianjin Medical University and the Tianjin Municipal Commission for Experimental Animal Control. In our study, 24 mongrel dogs of both sexes weighing 13 kg to 17 kg purchased from the Laboratory Animal Center of Tianjin Medical University were randomly assigned to a sham group (group S), paced control group (group C), paced + Ang-(1–7) group (group A), or a paced + Ang-(1–7) + A-71915 group (group N), six dogs in each group. The animals were anesthetized with pentobarbital sodium (30 mg•kg⁻¹) intravenously. Under aseptic technique, after intubation and mechanical ventilation, the distal end of a modified unipolar J pacing lead (St Jude Medical, MN, USA) was inserted into the right atrium through the right jugular vein. Initial atrial capture was verified with the use of an external stimulator (DF5A, Suzhou, China). Next, the proximal end of the pacing lead was connected to a programmable pacemaker (made in Shanghai Fudan University, China), which was inserted into a subcutaneous pocket in the neck. The atria in the paced control group, paced + Ang-(1–7) group and paced + Ang-(1–7) + A-71915 group were paced at 500 beats per minute (bpm) (120-ms cycle length) with the use of 0.2-ms square-wave pulses at twice-threshold current continuously for 14 days. The surface electrocardiogram (ECG) was examined to verify continuous 1:1 atrial capture on the first day and then every other day after operation in awake dogs. The pacemaker was implanted in the dogs in the sham group without pacing. Fresh wound dressings were changed for all dogs in each group every other day to avoid postoperative infection, and they were fed carefully. During the pacing, Ang-(1–7) (6 μg•kg⁻¹•h⁻¹) (Bachem AG, Bubendorf, Switzerland) or Ang-(1–7) (6 μg•kg⁻¹•h⁻¹) + A-71915 (ANP receptor antagonist, 0.30 μg•kg⁻¹•h⁻¹) (Bachem

AG, Bubendorf, Switzerland) were given intravenously through a jugular vein catheter by an ALZET[®] osmotic pump (DURECT Corporation, Cupertino, CA, USA) continuously during ARP for 14 days, respectively. Direct systolic blood pressure was measured during anesthesia before and after ARP for two weeks. Surface ECG and blood pressure were recorded by a multichannel physiological recorder (Model P4B533-K, China). The Ang-(1–7) dose was selected because 6 μg•kg⁻¹•h⁻¹ is verified as the highest dose that wouldn't affect blood pressure in our preliminary study (before and one hour after continuous Ang-(1–7) infusion the systolic blood pressures were 137±13 mm Hg vs 134±15 mm Hg, *p* > 0.05, *n* = 10). Studies by Shah et al.⁹ and us¹⁰ proved the ratio of A-71915 and Ang-(1–7) adopted for the present study optimum to block the beneficial effects of Ang-(1–7) for preventing cardiac antihypertrophy and atrial electrical remodeling induced by ARP.

Protocol of atrial ERPs measurement and AF induction

After the aforementioned operation for two weeks, each dog underwent an electrical examination. After intubation and mechanical ventilation under sterile technique, a median sternotomy was operated. Six pairs of electrodes (diameter: 1.5 mm and distance between poles: 1.5 mm) were sewn on the left and right atrial epicardium (LA and RA). The corresponding sites were at the high left and right atria (HLA and HRA), left and right atrial appendage (LAA and RAA) and low left and right atria (LLA and LRA). Saline was given intravenously by a jugular vein catheter, while systemic blood pressure was monitored through an arterial catheter inserted into the left femoral artery in each dog. In our study, we observed the changes in atrial ERPs, inducibility and duration of AF at basic pacing cycle lengths (BCLs) of 300 ms (BCL300), 250 ms (BCL250), and 200 ms (BCL200) at six aforementioned sites. When the atrial ERP was measured, the coupling interval of the extrastimulus (S2) at various BCLs was shortened in 2 ms steps and the longest coupling interval that failed to capture the atrium was defined as the ERP. AF induction was defined as P wave disappearance, rapid atrial activation with irregular ventricular response on atrial ECG after atrial programmed stimulation (S1–S2), which was attempted for three times at each site. The site where AF persisted longer than 1 second was denoted as an AF induction site. Then, the AF induction sites were excluded for atrial ERP analysis. Meanwhile, the duration of induced AF was recorded in each site.

Single-cell electrophysiological study

Cell isolation. After the electrical examination, the hearts were excised as soon as possible. Single cells were isolated from the LA by the methods developed in previous

studies.^{11,12} The excised hearts were immediately immersed in Tyrode's solution at room temperature. All solutions used for dissection and perfusion were equilibrated with 100% O₂. The left circumflex artery was cannulated, and the heart was immersed in Ca²⁺-free Tyrode's solution at 4°C for 5 minutes until the heartbeat stopped. Any leaking arterial branches were ligated with silk thread to ensure adequate perfusion. Then, the tissue was perfused at 25 ml/min with Ca²⁺-free Tyrode's solution for 20 minutes, followed by the same solution containing collagenase (100 U/ml, CLSII, Worthington Biochemical Corp., Lakewood, NJ, USA) and 0.5% bovine serum albumin (Sigma Chemical Co., St. Louis, MO, USA) for 40 minutes. Softened tissue was removed from a well-perfused region of the LA-free wall with forceps, triturated gently, and kept in a high-K⁺ storage solution at room temperature. Only quiescent rod-shaped cells with clear cross striations were selected. A small aliquot of the solution containing the isolated cells was placed in a 1-ml chamber mounted on the stage of an inverted microscope (Olympus Corp., Tokyo, Japan). Cells would adhere to the bottom of the chamber for 5 minutes and then be superfused at 3 ml/min with Tyrode's solution. Ionic currents were recorded 5 minutes after membrane rupture.

Solutions. Tyrode's solution contained (mmol/l) NaCl 136, KCl 5.4, MgCl₂ 0.8, CaCl₂ 1.8, NaH₂PO₄ 0.33, dextrose 10, and HEPES 10, pH 7.4 (adjusted with NaOH). The high-K⁺ storage solution contained (mmol/l) KCl 20, NaH₂PO₄ 10, dextrose 10, glutamic acid 70, taurine 10, and ethylene glycol tetraacetic acid (EGTA) 10, along with 0.5% albumin, pH 7.4 (adjusted with potassium hydroxide (KOH)).

The pipette solution for studying the L-type calcium current (I_{CaL}) contained (mmol/l) guanosine-5'-triphosphate (GTP) 0.1, CsCl 20, TEA-Cl 20, aspartic acid 80, CsOH 80, MgCl₂ 1, HEPES 10, EGTA 10, Mg₂ATP 5, Na₃GTP 0.1 and Na₂ phosphocreatine 5, pH 7.25 (adjusted with CsOH). The same pipette solution was used to study the inward Na⁺ exchange current (I_{Na}).

The extracellular solution for studying I_{CaL} was Tyrode's solution. The extracellular solution for studying I_{Na} contained (mmol/l) Choline-Cl 110, CsCl 20, MgCl₂ 1, HEPES 10, Glucose 10, NaCl 10 and CaCl₂ 1.8.

Data acquisition. The whole-cell patch-clamp technique was used with an Axopatch 200B amplifier (Axon Instruments, CA, USA) to record ionic currents in voltage-clamp mode. Borosilicate glass microelectrodes (1.5-mm outer diameter, 1.1-mm inner diameter) with tip resistances of 2.5 to 5 MΩ were used.

Resistance (Rs) was electrically compensated to minimize the duration of the capacitive surge on the current recording and the voltage drop across the clamped cell membrane. Precompensation Rs values averaged 6.9±0.8 MΩ. The mean Rs after compensation averaged 2.3±0.6 MΩ.

Membrane capacitance of the cells averaged 65.80±20.33 pF in the sham group ($n = 20$ cells), 68.24±20.00 pF in the paced control group ($n = 24$ cells), 63.40±13.68 pF in the paced + Ang-(1-7) group ($n = 22$ cells), and 60.12±15.87 pF in the paced + Ang-(1-7) + A-71915 group ($n = 26$ cells). To control the cell-size variability, the currents were expressed as densities (pA/pF).

Histology

Small portions of the left atrial free wall were excised and fixed for histological analysis. Tissue fibrosis was evaluated by Masson's trichrome staining. Microscopic images were analyzed with Motic Images Advanced 3.2 software. Connective tissue was identified according to its color, and a percentage of the fibrotic tissue area was recorded to express the degree of fibrosis. These analyses were performed by a pathologist unaware of the treatment.

Total RNA preparation and quantitative analysis by real-time reverse transcription polymerase chain reaction (real-time RT-PCR)

After the electrophysiological studies, the left atrium was cut off and used for molecular biological studies. Specimens were rapidly frozen in liquid nitrogen and stored separately at -80°C for further analysis. One aliquot of each tissue sample was used to investigate the messenger RNA (mRNA) expression of transforming growth factor (TGF)-β₁ and ANP. In brief, 100 mg of tissue was homogenized in 1 ml of TRIzol reagent (Life Technology of Thermo Fisher Scientific Inc, MA, USA) extracted with chloroform and precipitated in isopropyl alcohol. Total RNA was incubated in DNase I (0.2U/μl, Invitrogen, Carlsbad, CA, USA) for 30 minutes, extracted by phenol-chloroform, precipitated in isopropyl alcohol, and subsequently dissolved in diethylpyrocarbonate (DEPC)-treated water. The integrity of each sample was checked on a denaturing agarose gel. The concentration of total RNA was determined spectrophotometrically to be pure if a ratio of optical density (OD) 260:280 > 1.6. Samples were stored at -80°C until used for real-time RT-PCR analysis.

Specific oligonucleotide primer pairs used for amplification of TGF-β₁ and ANP genes were designed according to the sequences obtained from GenBank. GenBank accession numbers were [NM 001003309](#) (TGF-β₁), [XM 845264](#) (ANP), and [NM 001003142.1](#) (glyceraldehyde-3-phosphate dehydrogenase (GADPH)). The primers specific for each protein were: 5'- CCTGCTGAGGCTCAAGTTAAA/5'-ACATCAAAGGACAGCCATTCT (TGF-β₁), 5'-GAGGCAGGATGGATAGGATTG/5'-CCGTGGTGCTGAGTTTATTG (ANP), and 5'- GGCGTGAACCATGAGAAGTAT/5'-GTGGAAGCAGGGATGATGTT (GADPH). mRNA was transcribed into complementary DNA (cDNA) by TaqMan Reverse Transcription Reagents Kit. Relative mRNA expression values analyses were

Table 1. Hemodynamic parameters before and after pacing in each group ($\bar{x} \pm s$).

Groups	Heart rate (bpm)			Systolic blood pressure (mm Hg)		
	Before pacing	After pacing	<i>p</i>	Before pacing	After pacing	<i>p</i>
S	186±13	186±15	>0.05	143±8	144±9	>0.05
C	189±11	187±16	>0.05	142±9	145±13	>0.05
N	182±12	184±9	>0.05	142±13	145±12	>0.05
A	186±10	187±12	>0.05	145±13	146±9	>0.05
F	0.38	0.07		0.09	0.02	
P	>0.05	>0.05		>0.05	>0.05	

S: sham group; C: paced control group; N: paced+ Ang-(1-7) + A-71915 group; A: paced + Ang-(1-7); F: variance ratio; P: P-value.

validated by real-time RT-PCR with SYBR Green (TAKARA Biotechnology Co., Ostu, Shiga, Japan). Efficiency of the amplification reaction or potential variation in RNA loading was corrected by the expression of GAPDH as endogenous control. The corresponding PCR products were 98 bp and 110 bp, respectively. The real-time RT-PCR consisted of 40 cycles of 95°C for 15 seconds, 57°C for 30 seconds and 72°C for 32 seconds. Relative expression values were calculated as previously described.^{13,14} The expression level of GAPDH was used as an internal control.

Protein extraction and sodium dodecyl sulfate-polyacrylamide gel electrophoresis (SDS-PAGE) and Western blotting

The left atrium (0.1 g/sample) was lysed in a homogenization buffer for 15 minutes at 35°C using the delipidation method as previously described. Protein extracts from the left atrium were prepared with M-PER Mammalian Protein Extraction Reagent (Thermo Fisher Scientific Pierce, IL, USA) and quantified with BCA Protein Assay Kit (Thermo Fisher Scientific Pierce, IL, USA).

In brief, protein electrophoresis was performed on 10% Tri-HCl polyacrylamide-ready gel and electroblotted onto Hybond-C extra nitrocellulose membranes. Membranes were incubated with antibody against TGF- β_1 (Abcam, Cambridge, UK), ANP (Abcam, Cambridge, UK), and β -actin (Abcam, Cambridge, UK). Then, membranes were incubated with the secondary antibody. Proteins were visualized by chemiluminescence using the ECLTM Western blotting system and the signals were detected and recorded by autoradiography. The concentration of target proteins was determined by signal intensity (integral volume) of the appropriate bands on autoradiogram analyzed by a scanner and Quantity One software.

Statistical analysis

All data are expressed as mean±SD. Statistical comparisons among groups were performed with analyses of

variance (ANOVAs). If significant effects were indicated by ANOVA, a *t* test with Bonferroni's correction or Dunnett's test was used to evaluate the significance of differences between individual mean values. Inducible rate of AF was analyzed with exact probability test and duration of AF was compared by Wilcoxon rank sum test. A two-tailed $p < 0.05$ was taken to indicate statistical significance.

Results

Hemodynamic parameters

As summarized in Table 1, there was no significant difference in ventricular rate or systolic blood pressure between groups at baseline ($p > 0.05$) and no difference was found after ARP for two weeks ($p > 0.05$), while the heart rate and blood pressure were not affected by ARP in each group ($p > 0.05$).

Atrial ERPs at various BCLs

In the paced control group, atrial ERPs of the six atrial sites at BCL300, BCL250 and BCL200 were shortened significantly compared with the sham group ($p < 0.05$). In group A the shortening of atrial ERPs in most of the atrial sites was attenuated by Ang-(1-7) treatment at various BCLs compared with the animals in the paced control group ($p < 0.05$). The atrial ERPs of the dogs treated by A-71915 showed no difference compared with the paced control group ($p > 0.05$) (Figure 1(a)–(c)).

Inducibility and duration of AF

There were overall 36 sites in the six dogs in each group, where six atrial sites in each dog were used to record electrophysiological data and induce AF. Compared with the sham group, the inducible rate of AF was elevated at various BCLs in the paced control group ($p < 0.05$). However, the increasing of inducibility and duration of AF was attenuated after Ang-(1-7) treatment at various BCLs, compared with the paced control group ($p < 0.05$). The inducibility and duration of AF in the group treated by

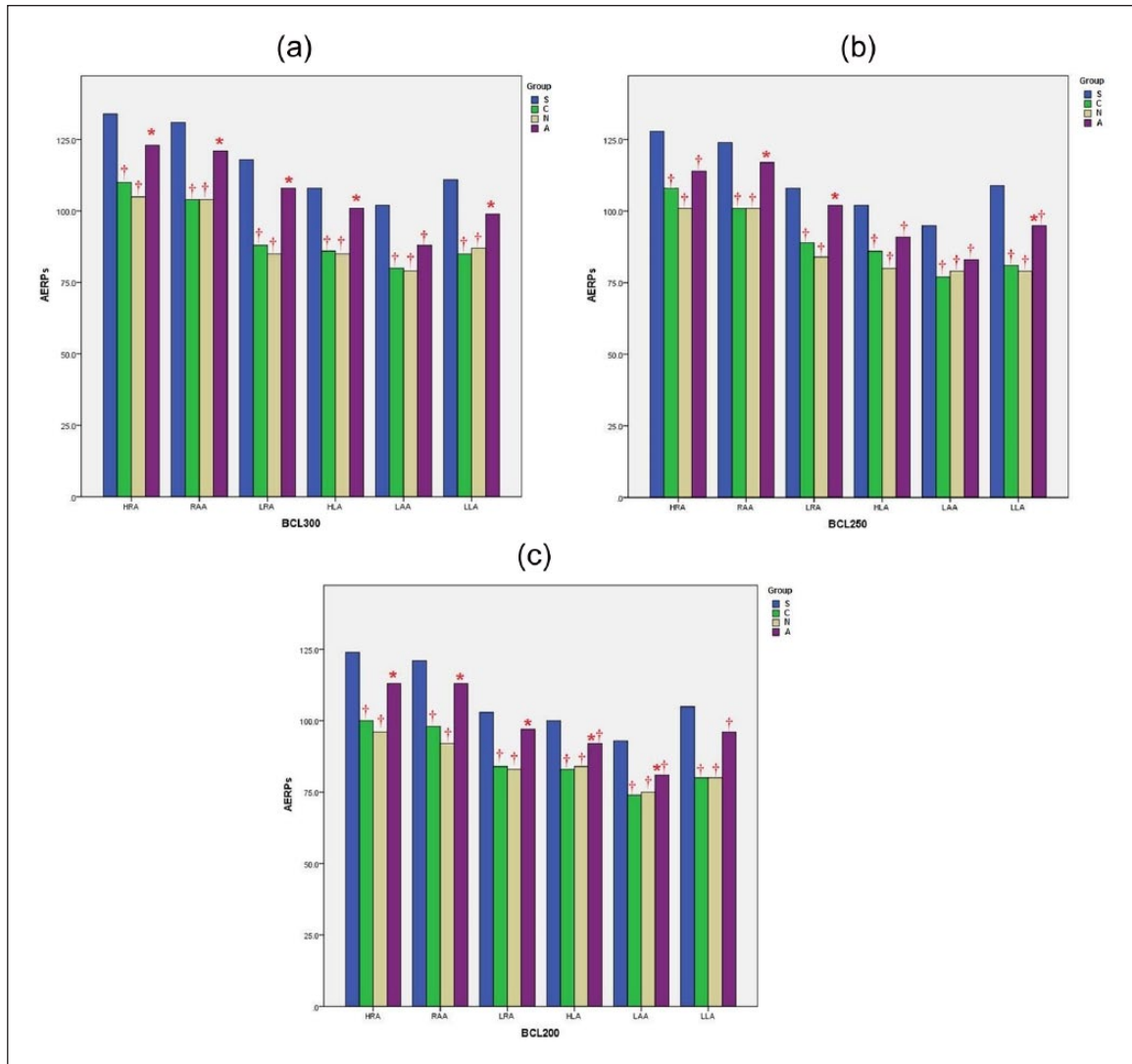


Figure 1. (a) At BCL300, the atrial ERPs of six sites were shortened significantly in the paced control group compared with the sham ($\dagger p < 0.05$). After Ang-(1-7) treatment, the shortening of atrial ERPs was attenuated except at LAA compared with the paced control group ($*p < 0.05$). The atrial ERPs of the dogs treated by A-71915 showed no difference compared with the paced control group ($p > 0.05$). (b) At BCL250, the atrial ERPs of six sites were shortened in paced control group compared with the sham ($\dagger p < 0.05$). The shortening of atrial ERPs in Ang-(1-7)-treated dogs was attenuated except at the HRA, HLA and LAA compared with the paced control group ($*p < 0.05$). The atrial ERPs of the dogs treated by A-71915 showed no difference compared with the paced control group ($p > 0.05$). (c) At BCL200, the atrial ERPs of six sites were shortened in the paced control group compared with the sham ($\dagger p < 0.05$). The shortening of atrial ERPs in Ang-(1-7)-treated dogs was attenuated except at the LLA compared with the paced control group ($*p < 0.05$). The atrial ERPs of the dogs treated by A-71915 showed no difference compared with the paced control group ($p > 0.05$). BCL: basic pacing cycle; ERPs: effective refractory periods; HRA: high right atria; HLA: high left atria; LAA: left atrial appendage; LLA: low left atria; AERPs: atrial effective refractory periods; Ang-(1-7): Angiotensin-(1-7); S: sham group; C: paced control group; A: paced + Ang-(1-7); N: paced + Ang-(1-7) + A-71915 group.

A-71915+Ang-(1-7) showed no difference compared with the paced control group ($p > 0.05$) (Table 2).

Pathological examination

Typical histological sections from each group are shown in Figure 2(a)–(d). Interstitial fibrosis is shown in blue by Masson trichrome staining. Atrial tissue from the sham

dogs appeared normal. In contrast, atrial tissue from the dogs in the paced control group and A-71915+Ang-(1-7) group showed obvious interstitial fibrosis spreading throughout the tissue. In addition, atrial myocytes of heterogeneous size and arrangement were found in these tissues. These pathological abnormal findings were attenuated in the Ang-(1-7) group. A quantitative analysis to evaluate atrial fibrosis is shown in Figure 2(e). The

percentage of fibrosis in the left atria in the Ang-(1-7) group was significantly lower than that in the paced control group ($5\pm 1\%$ vs $18\pm 1\%$, $p < 0.01$), but was higher than

that in the sham group ($5\pm 1\%$ vs $2\pm 1\%$, $p < 0.01$). There was no statistical difference between the paced control group and the A-71915+Ang-(1-7) group.

Table 2. The inducibility and duration of AF in each group at various BCLs.

Groups	BCL300ms		BCL250ms		BCL200ms	
	Ic	Dr	Ic	Dr	Ic	Dr
S	1/30		0	0	1/30	
C	14/30 ^a	45±12 ^a	11/30 ^a	46±15 ^a	13/30 ^a	48±12 ^a
N	12/30 ^a	47±14 ^a	11/30 ^a	50±15 ^a	13/30 ^a	44±11 ^a
A	3/30 ^b	11±4 ^b	3/30 ^b	13±5 ^b	4/30 ^b	10±3 ^b

AF was induced at six sites in each heart; six dogs and overall 36 sites were studied in each group. Ic: Sites where AF was induced. Dr: Average duration of induced AF ($\bar{x} \pm s$, second). Ic and Dr were increased significantly in the paced control group at various BCLs (vs sham, ^a $p < 0.05$). In Ang-(1-7)-treated dogs, the increasing of Ic and Dr was attenuated compared to paced control group (^b $p < 0.05$). However, the Ic and Dr in the groups treated by A-71915+Ang-(1-7) showed no difference to the paced control group ($p > 0.05$). Ang-(1-7): Angiotensin-(1-7); BCL: basic pacing cycle length. AF: atrial fibrillation. S: sham group; C: paced control group; N: paced+ Ang-(1-7) + A-71915 group; A: paced + Ang-(1-7).

I_{Na} changes

Figure 3 illustrates the overall results for I_{Na} current densities. Depolarizing 100-ms pulses ranging from -80 mV to $+60$ mV elicited I_{Na} in atrial myocytes in dogs. I_{Na} density was markedly decreased without any changed form of the current-voltage (I-V) curve in the paced control group. The decreasing of maximum peak I_{Na} density was obviously prevented after Ang-(1-7) treating compared with paced control group. But statistical differences were not found in the maximum peak I_{Na} density between the paced control group and the paced + Ang-(1-7) + A-71915 group. Maximum peak I_{Na} density averaged -48.67 ± 20.04 pA/pF in the sham group ($n = 11$ cells), -30.26 ± 9.13 pA/pF in the paced control group ($n = 12$ cells, $p < 0.05$ vs sham), -43.13 ± 14.83 pA/pF in the paced + Ang-(1-7) group ($n = 8$ cells, $p < 0.05$ vs control), -32.29 ± 9.82 pA/pF in paced + Ang-(1-7) + A-71915 group ($n = 9$ cells, $p > 0.05$ vs control), respectively.

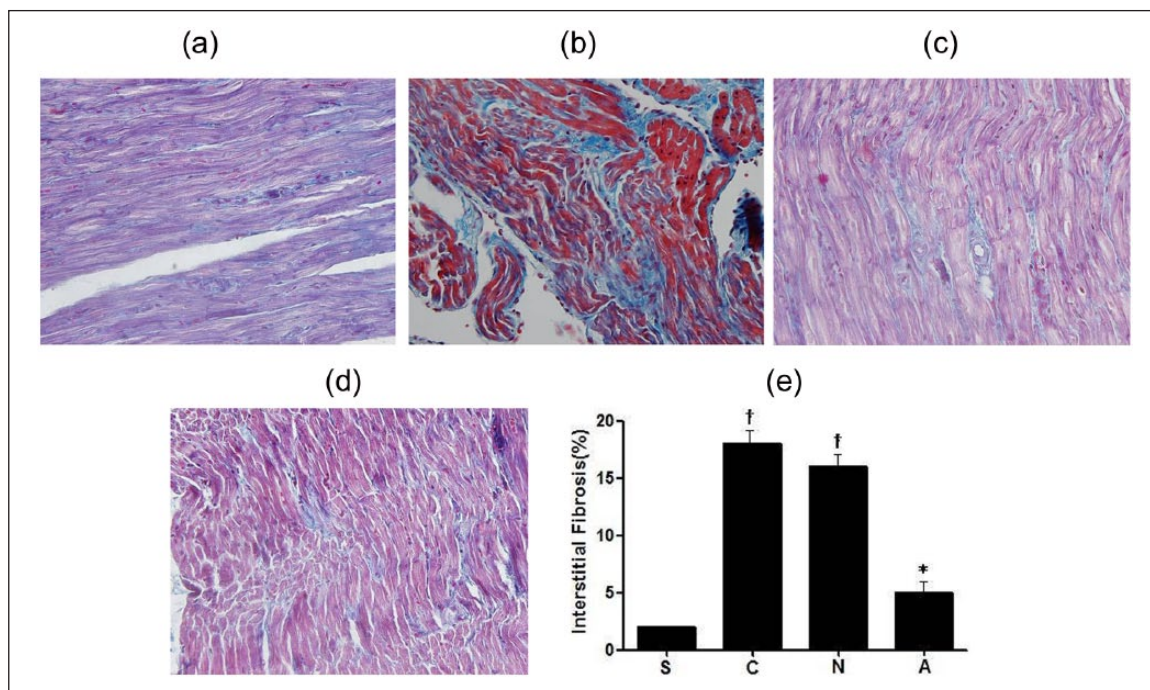


Figure 2. Panels 2(a)–(d) show the representative histologic sections of the left atrial free wall from a sham dog (a), paced control dog (b), Ang-(1-7)-treated dog (c) and Ang-(1-7)+A-71915-treated dog (d). Interstitial fibrosis is shown in blue by Masson trichrome staining. Atrial tissue from the sham dog appeared normal. Extensive interstitial fibrosis can be seen in the paced control dog, but is attenuated in the Ang-(1-7)-treated dog. There was no statistical difference between the paced control group and the A-71915+Ang-(1-7) group ($\times 200$; Masson trichrome staining). (e) A quantitative analysis to evaluate atrial fibrosis. The percentage of fibrosis in the left atria in the Ang-(1-7) group was significantly lower than that in the paced control group, but was higher than that in the sham group ($p < 0.01$). There was no statistical difference between the paced control group and the A-71915+Ang-(1-7) group. S: sham group; C: paced control group; A: paced + Ang-(1-7); N: paced+ Ang-(1-7) + A-71915 group; Ang-(1-7): Angiotensin-(1-7). † $p < 0.01$ compared with the sham group, * $p < 0.01$ compared with the paced group.

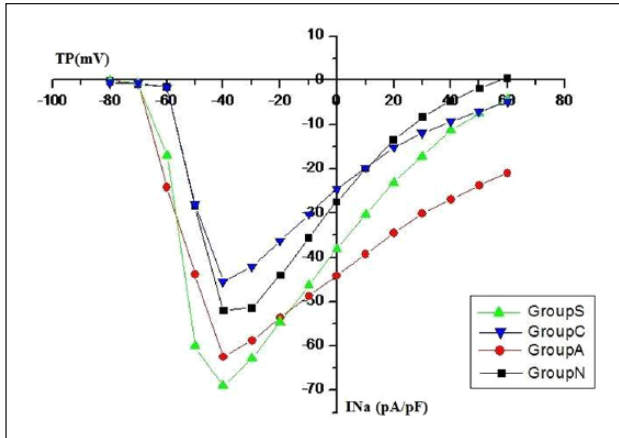


Figure 3. Overall results for I_{Na} current densities. Depolarizing 100-ms pulses from -80 mV elicited I_{Na} in atrial myocytes from dogs. I_{Na} density was significantly decreased in paced group. Although I_{Na} density decreased in paced dogs, the form of the I-V curve did not change. The reduction of maximum I_{Na} density was significantly prevented by Ang-(1-7) compared with the paced control group ($p < 0.05$). But no significant differences were found in I_{Na} density between the paced control group and the paced + Ang-(1-7) + A-71915 group. I_{Na} : inward Na^+ exchange current; Ang-(1-7): Angiotensin-(1-7); S: sham group; C: paced control group; A: paced + Ang-(1-7); N: paced + Ang-(1-7) + A-71915 group; I-V: current-voltage.

I_{CaL} changes

Any accumulative effect on I_{CaL} attenuation was minimized when waiting for 5 minutes after membrane rupture in our study.

Figure 4 illustrates the overall results for I_{CaL} current densities. Depolarizing 200-ms pulses ranging from -50 mV to $+50$ mV elicited typical I_{CaL} . The density of I_{CaL} was significantly decreased by ARP for 14 days. Maximum peak I_{CaL} density averaged -3.64 ± 1.06 pA/pF in the paced control group ($n = 8$ cells) was decreased compared with -7.12 ± 1.23 pA/pF in the sham group ($n = 9$ cells) ($p < 0.05$). The maximum peak density of I_{CaL} in the paced + Ang-(1-7) group (-6.17 ± 1.61 pA/pF, $n = 7$ cells) was significantly higher than that in paced control group ($p < 0.05$), but the maximum peak density of I_{CaL} in the paced + Ang-(1-7) + A-71915 group (-4.30 ± 0.99 pA/pF, $n = 6$ cells) showed no changes compared with the paced control group ($p > 0.05$).

Expression of $I_{Nav1.5}$ subunit ($Nav1.5\alpha$), $Cav1.2$, $TGF-\beta_1$ or ANP mRNA

Figure 5(a)–(d) shows the relative mRNA expression values of $Nav1.5\alpha$, $Cav1.2$, $TGF-\beta_1$ or ANP mRNA in six hearts (one independent determination per heart) from the dogs in each group. In the paced control group, the expression of $Nav1.5\alpha$ and $Cav1.2$ mRNA was decreased

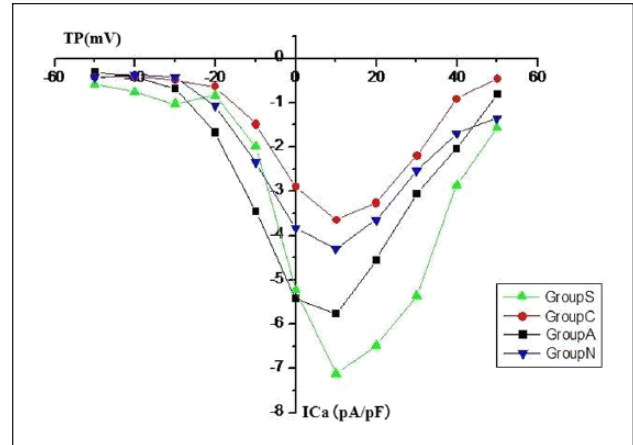


Figure 4. Overall results for I_{CaL} current densities. Depolarizing 200-ms pulses ranging from -50 mV to $+50$ mV elicited typical I_{CaL} . After 14 days of atrial pacing, I_{CaL} density was significantly reduced in the paced control group ($p < 0.05$). The decreasing of I_{CaL} density in the paced + Ang-(1-7) group was obviously attenuated compared with that in the paced control group ($p < 0.05$), but the density of I_{CaL} in the paced + Ang-(1-7) + A-71915 group was not changed compared with the paced control group ($p > 0.05$). I_{CaL} : L-type calcium current; Ang-(1-7): Angiotensin-(1-7); S: sham group; C: paced control group; A: paced + Ang-(1-7); N: paced + Ang-(1-7) + A-71915 group.

significantly after 14 days of ARP ($p < 0.05$ vs sham). The decreasing of $Nav1.5\alpha$ and $Cav1.2$ mRNA expression was attenuated by Ang-(1-7) treatment ($p < 0.05$). $TGF-\beta_1$ or ANP mRNA expression was increased in the paced control group ($p < 0.05$ vs sham). The increasing of $TGF-\beta_1$ mRNA expression was attenuated in the Ang-(1-7) group ($p < 0.05$). The increasing of ANP mRNA expression was amplified in the Ang-(1-7) group and the A-71915+Ang-(1-7) group ($p < 0.05$). There was no significant difference in the expression of $Nav1.5\alpha$, $Cav1.2$ or $TGF-\beta_1$ mRNA between the paced control group and the A-71915+Ang-(1-7) group.

ANP or $TGF-\beta_1$ changes in protein level

Lanes S, C, N and A shows the protein expression values of ANP or $TGF-\beta_1$ in the sham group, paced control group, paced+Ang-(1-7)+A-71915 or paced+Ang-(1-7) group, by the method of Western blotting, respectively (Figure 6). ANP or $TGF-\beta_1$ expression was increased in the paced control group ($p < 0.05$ vs sham). The increasing of ANP protein expression was amplified in the Ang-(1-7) group and A-71915+Ang-(1-7) group ($p < 0.05$). The increasing of $TGF-\beta_1$ protein expression was attenuated by Ang-(1-7) treatment ($p < 0.05$). There was no statistical difference in the protein expression of $TGF-\beta_1$ between the paced control group and the paced + Ang-(1-7) + A-71915 group ($p > 0.05$).

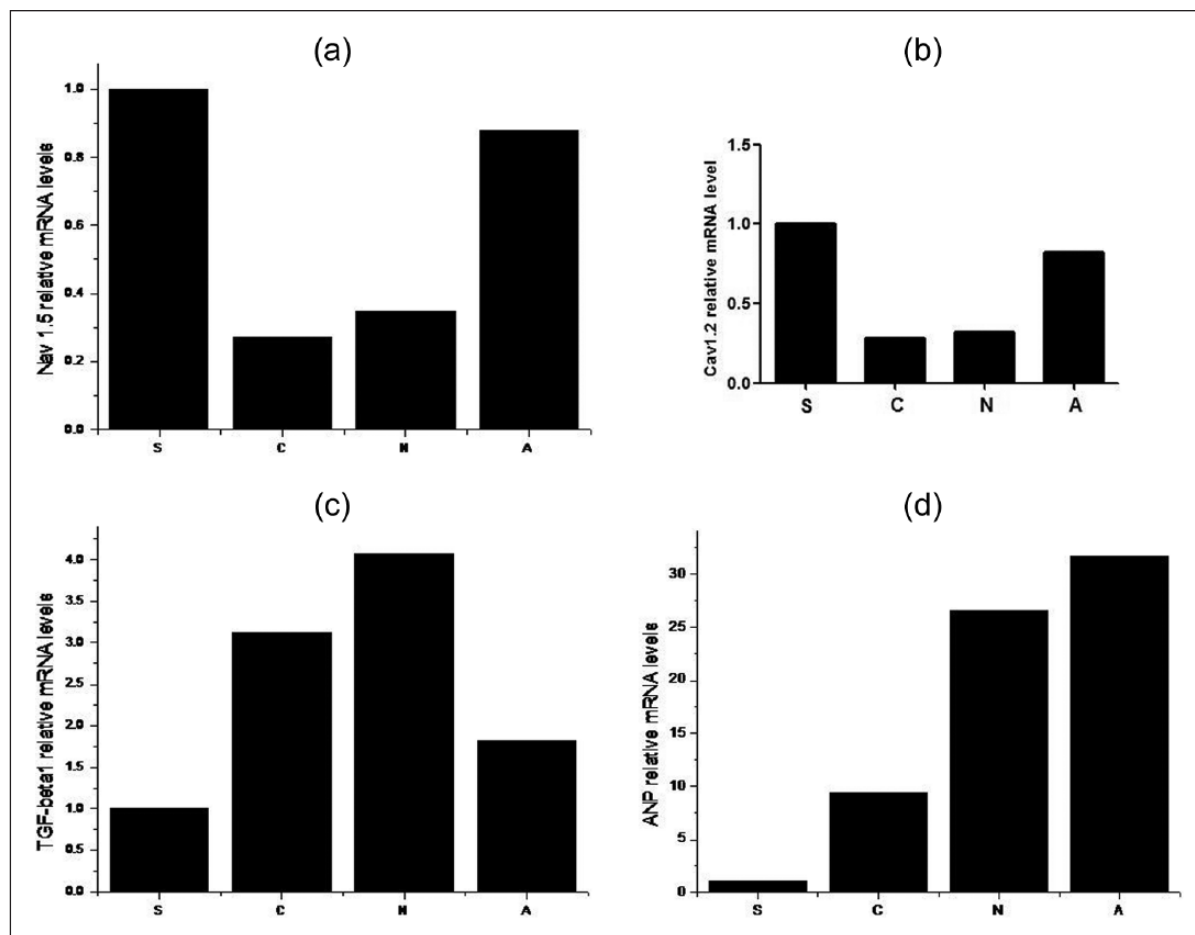


Figure 5. Relative mRNA expression values of Nav1.5 α (a), Cav1.2 (b), TGF- β_1 (c) or ANP (d) mRNA in six hearts (one independent determination per heart) from each group of dogs. In the paced control group, Nav1.5 α and Cav1.2 mRNA expression were decreased significantly after 14 days of atrial rapid pacing ($p < 0.05$ vs sham). The decreasing of Nav1.5 α and Cav1.2 mRNA expression was attenuated by Ang-(1-7) treating ($p < 0.05$). TGF- β_1 or ANP mRNA expression was increased in the paced control group ($p < 0.05$ vs sham). The increasing of TGF- β_1 mRNA expression was attenuated by Ang-(1-7) treatment ($p < 0.05$), but the increasing of ANP mRNA expression was amplified in the Ang-(1-7) group and the A-71915+Ang-(1-7) group ($p < 0.05$). There was no statistical difference in the expression of Nav1.5 α , Cav1.2, or TGF- β_1 mRNA between the paced control group and the A-71915+Ang-(1-7) group. mRNA: messenger RNA; TGF- β_1 : transforming growth factor β_1 ; ANP: atrial natriuretic peptide; Ang-(1-7): Angiotensin-(1-7).

Discussion

RAS has been proved to participate in several cardiovascular diseases, including hypertension, myocardial infarction, cardiomyopathy, arrhythmias and so on. In the latest two decades, another heptapeptide, Ang-(1-7) transformed from Ang I and/or Ang II, as a novel member of RAS has been focused on because of its excitingly protective roles in the cardiovascular system such as vasodilation and anti-trophic effects.^{15,16} Research has also investigated the related signaling pathway mediating the beneficial effects of Ang-(1-7) on the heart. A recent study suggested that Ang-(1-7) prevented cardiac electrical remodeling through increasing ANP secretion mediated by Mas/PI3K/Akt/NO signaling pathway *in vitro*⁹ in accordance with our previous study *in vivo*.¹⁰ In our previous study, after two-hour

ARP in a canine model, Ang-(1-7) promoted the increasing of atrial ANP concentration and prevented atrial electrophysiological abnormality including the shortening of atrial ERPs and the increasing of AF vulnerability induced by ARP through the Mas/PI3K/Akt/NO axis. ANP was suggested to participate in the beneficial effects of Ang-(1-7) by preventing electrical remodeling induced by ARP.¹⁰ However, the aforementioned results were obtained only in the acute pacing atria of dogs in our previous study; the ionic channel function, the related protein and gene expression, and the atrial histopathological characteristics were not as easily affected in an acute ARP model.^{9,17} Thus, in the present study, a canine model of ARP for two weeks was established to find more evidence on the changes of ionic channel function, the related protein and

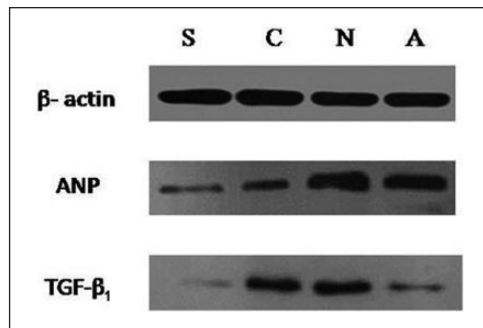


Figure 6. Lanes S, C, N and A show the protein expression values of ANP or TGF- β_1 in the sham group, paced control group, paced + Ang-(1-7) + A-71915 or paced + Ang-(1-7) group, by the method of Western blotting, respectively. ANP or TGF- β_1 expression was increased in the paced control group ($p < 0.05$ vs sham). The increasing of ANP expression was amplified in the Ang-(1-7) group and A-71915+Ang-(1-7) group ($p < 0.05$), but the increasing of TGF- β_1 protein expression was attenuated by Ang-(1-7) treatment ($p < 0.05$). There was no statistical difference in the protein expression of TGF- β_1 between the paced control group and the paced + Ang-(1-7) + A-71915 group. TGF- β_1 : transforming growth factor β_1 ; ANP: atrial natriuretic peptide; Ang-(1-7): Angiotensin-(1-7); S: sham group; C: paced control group; A: paced + Ang-(1-7); N: paced+ Ang-(1-7) + A-71915 group.

gene expression, and atrial histopathological characteristics to clarify the potential role of ANP in the effects of Ang-(1-7) on atrial remodeling. The present results indicated that: 1) Ang-(1-7) augmented the increasing of atrial ANP secretion in gene and protein levels induced by ARP. 2) Ang-(1-7) alleviated the electrophysiological abnormality including the shortening of atrial ERPs and the increasing of AF vulnerability. Furthermore, Ang-(1-7) attenuated the decreasing of I_{CaL} and I_{Na} densities, and the decreasing of related channel protein expression. 3) Ang-(1-7) suppressed TGF- β_1 expression and atrial fibrosis observed in Masson trichrome staining induced by ARP. 4) The aforementioned roles of Ang-(1-7) were blocked by the antagonist of ANP. Thus, ANP played a crucial role in the beneficial effects of Ang-(1-7) on atrial remodeling.

Effects of Ang-(1-7) on atrial remodeling induced by ARP

Effects of Ang-(1-7) on atrial ERPs, AF vulnerability and ionic changes. ARP is an effective stimulus to induce atrial remodeling.¹⁸ Nakashima and Kumagai¹⁹ showed in dogs after ARP for two weeks, atrial ERPs were shortened coupled with the increasing of intra-atrial conduction times (CTs) and duration of induced AF. This agreed with our previous and present studies, and was proved to be related to AF development and maintenance. Ang-(1-7) was shown to attenuate the shortening of atrial ERPs and the increasing of AF vulnerability after ARP in our previous

and present study, which was related to some ionic changes. The densities of I_{TO} , I_{CaL} and I_{Na} and the expression of related ionic channel subunits genes were depressed by ARP while Ang-(1-7) prevented the depression of I_{TO} , I_{CaL} and I_{Na} mRNA expression.²⁰ Thus, atrial remodeling induced by ARP is associated with characteristic ionic remodeling. According to a report from Yue et al.,²¹ ARP induced the decreasing of action potential duration (APD) and APD adaptation to the rate of the atrial myocytes. The densities of I_{TO} and I_{CaL} in the atria were decreased coupled with the duration of rapid pacing increasing. After ARP for one week, the concentration of I_{TO} Kv4.3 and I_{CaL} α_1C subunit mRNA was reduced by 60% and 57%, respectively. The protein expression for Kv4.3 was decreased in accordance with the changes of mRNA and I_{TO} (I_{TO} refers to transient outward current).²¹ According to another report from the same research group, the downregulation of the L-type Ca^{2+} channel gene in AF was demonstrated to be coupled with the densities of the I_{CaL} channel through dihydropyridine receptor binding assays.²² These results indicated that chronic ARP altered the expression of atrial ion channel in gene and protein levels to result in the related current changes. The aforementioned abnormality of the ion channel encouraged the occurrence of AF. It was implied that Ang-(1-7) attenuated the aforementioned electrical and ionic remodeling induced by ARP to prevent the occurrence of AF.

Effects of Ang-(1-7) on AF. As is believed, chronic atrial tachycardia results in atrial structural remodeling, mainly including atrial fibrosis and hypertrophy, which participate in the initiation and maintenance of AF.²³⁻²⁶ In our experiment, ARP for 14 days induced extensive interstitial fibrosis in the atria of the paced control group, but Ang-(1-7) treatment significantly reduced the percentage of interstitial fibrosis compared with the paced control group. The difference in atrial fibrosis between the two groups was in accordance with the changes of TGF- β_1 expression, which were shown to be elevated after ARP but decreased after Ang-(1-7) treatment. According to recent reports, TGF- β_1 was accepted as a profibrotic molecule that played a critical role in atrial fibrosis pathways and also predicted the success of AF ablation procedure.²⁷ In hypertensive patients with AF, TGF- β_1 was confirmed to be independently correlated with left atrial diameter and the presence of AF.²⁸ Moreover, in the latest study by Canpolat et al., higher levels of TGF- β_1 were proved to be associated with more extensive LA fibrosis, which predicted worse outcomes in patients undergoing cryoablation for lone AF.²⁹ Thus, it is suggested that Ang-(1-7) prevented the increasing of TGF- β_1 expression to attenuate atrial fibrosis induced by ARP.

The potential role of ANP in the effects of Ang-(1-7) on atrial electrical and structural remodeling induced by ARP. In our

present and previous experiments, ANP secretion has been proved to be increased in the atria from the paced control group after ARP for two hours and two weeks. Much clinical research supported our results. A recent study reported that atrial and circulating ANP concentration was increased in patients with paroxysmal and persistent AF.³⁰ ANP was referred to be a predictive factor of AF recurrence during 12 months post-cardioversion.³¹ Thus, it indicated that the increasing of ANP secretion was related to atrial tachycardia, both in animal experiments and clinical research. As is known, increasing atrial wall tension is accepted as a crucial stimulus for atrial ANP secretion.³² It was revealed that the volume of left atria was increased in patients with paroxysmal AF.³³ In addition, the promotion of Ang-(1–7) on ANP secretion after ARP was independent of hemodynamic changes in the present study.

In our previous and present studies, Ang-(1–7) was proved to prevent atrial structural and electrical remodeling induced by ARP. The related mechanism of Ang-(1–7) had been investigated recently. Several reports have clarified that Ang-(1–7) can depress cardiac remodeling by selectively binding to cardiomyocytes *in vitro* and *in vivo*. But in mice with deficient Mas receptor, Ang-(1–7) wasn't able to bind to cardiomyocytes.³⁴ Furthermore, Ang-(1–7) was confirmed to be able to activate nitric oxide synthase and NO generation through the PI3K/Akt pathway in adult ventricular cardiomyocytes.³⁵ Thus, the Mas/PI3K/Akt/NO axis was accepted as the indispensable signaling pathway of Ang-(1–7). In isolated pacing atria of the rat, the antagonists of different sections in the Mas/PI3K/Akt/NO axis were observed to depress ANP secretion encouraged by Ang-(1–7).⁹ In our previous acute ARP canine model, the antagonists of the Mas/PI3K/Akt/NO axis including Mas receptor antagonist (A-779), PI3K inhibitor (wortmannin), Akt/protein kinase B inhibitor (API-2) and NO synthase inhibitor (L-NAME) were proved to block the effects of Ang-(1–7) on both atrial electrical remodeling and the secretion of atrial ANP after ARP. ANP receptor antagonist A-71915 was observed to inhibit the beneficial effects of Ang-(1–7) on atrial electrical remodeling induced by ARP.¹⁰ Furthermore, in the present chronic ARP canine model, A-71915 was proved to block the effects of Ang-(1–7) on preventing atrial fibrosis and inhibiting the changes of I_{CaL} , I_{Na} and the related channel genes expression. Correspondingly, in Yoshida's study, ANP was proved to attenuate the shortening of the atrial ERPs and atrial monophasic action potential (MAP) duration induced by ARP for seven hours.¹⁷ Miao et al.³⁶ reported that ANP depressed action potentials and inhibited basal I_{CaL} through the cyclic guanosine monophosphate (cGMP)/phosphodiesterase (PDE)2/cyclic adenosine monophosphate (cAMP) pathway on developmental cardiomyocytes. Meantime, ANP antifibrotic properties have been shown in cardiomyocytes or in induced cardiac myofibroblasts (Ang II-

induced differentiation). In the study by Fujita et al., ANP administration to rats significantly reversed Ang II-induced myocyte hypertrophy and fibrosis by attenuating inflammation, at least partly through endothelin 1/endothelin receptor A cascade.³⁷ Additionally, another research reported that in a human adrenocortical cell line (NCI-H295R), ANP attenuated Ang II-induced aldosterone synthesis to prevent cardiac remodeling.³⁸ According to a recent report, in isolated rat cardiac fibroblasts, ANP itself was proved to decrease the proliferation rate and collagen secretion significantly mediated by the ANP/natriuretic peptide receptor A (NPRA)/cGMP signaling system.³⁹ It was suggested that ANP inhibited adverse cardiac remodeling by preventing cardiomyocyte hypertrophy and fibrosis based on G kinase activation in experiments using cultured cells and NPRA-deficient mice.⁴⁰ The aforementioned findings and our results indicated that ANP played crucial roles in the beneficial effects of Ang-(1–7) on atrial electrical and structural remodeling induced by ARP. Thus, Ang-(1–7) prevented atrial electrical and structural remodeling induced by ARP mediated by the Mas/PI3K/Akt/NO/ANP signaling pathway in an atrial tachycardia canine model.

Study limitations

First, the ventricular rate was not controlled by blocking the atrioventricular (AV) node and the ventricular function was not evaluated by echocardiography in our present study. But the ventricular rate and blood pressure were not obviously affected by ARP in each group, so left ventricular dysfunction evoked by ventricular tachycardia might not contribute to atrial remodeling in the chronic rapid atrial-pacing model. On the other hand, maintenance of physiological AV conduction resembled the situation of the patients with AF. Second, the electrophysiological examination may slightly affect the detection of the related protein and gene expression of ionic channel subunits ANP and TGF- β_1 in the left atria. But the same method to determine these electrophysiological parameters was adopted in the four groups. Thus, the electrophysiological examination itself wouldn't affect the final results of our study.

Conclusions

In a chronic ARP canine model, Ang-(1–7) inhibited atrial electrical and structural remodeling. The aforementioned beneficial effects of Ang-(1–7) were participated in by ANP, maybe as the crucial downstream factor of the Mas/PI3K/Akt/NO signaling pathway.

Declaration of Conflicting Interests

The author(s) declared no potential conflicts of interest with respect to the research, authorship and/or publication of this article.

Funding

The author(s) disclosed receipt of the following financial support for the research, authorship, and/or publication of this article: This work was supported by the Program of Natural Science Foundation of China (No. 81100131) and the Specialized Research Fund for the Doctoral Program of Higher Education of China (No. 20111202120008).

References

1. Tsai CT, Lai LP, Lin JL, et al. Renin-angiotensin system gene polymorphisms and atrial fibrillation. *Circulation* 2004; 109: 1640–1646.
2. Caron KM, James LR, Kim HS, et al. Cardiac hypertrophy and sudden death in mice with a genetically clamped renin transgene. *Proc Natl Acad Sci U S A* 2004; 101: 3106–3111.
3. Li D, Shinagawa K, Pang L, et al. Effects of angiotensin-converting enzyme inhibition on the development of the atrial fibrillation substrate in dogs with ventricular tachypacing-induced congestive heart failure. *Circulation* 2001; 104: 2608–2614.
4. Schiavone MT, Santos RA, Brosnihan KB, et al. Release of vasopressin from the rat hypothalamo-neurohypophysial system by angiotensin-(1–7) heptapeptide. *Proc Natl Acad Sci U S A* 1988; 85: 4095–4098.
5. Santos RA, Castro CH, Gava E, et al. Impairment of in vitro and in vivo heart function in angiotensin-(1–7) receptor MAS knockout mice. *Hypertension* 2006; 47: 996–1002.
6. Grobe JL, Mecca AP, Lingis M, et al. Prevention of angiotensin II-induced cardiac remodeling by angiotensin-(1–7). *Am J Physiol Heart Circ Physiol* 2007; 292: 736–742.
7. Ferrario CM. Angiotensin-converting enzyme 2 and angiotensin-(1–7): An evolving story in cardiovascular regulation. *Hypertension* 2006; 47: 515–521.
8. Donoghue M, Hsieh F, Baronas E, et al. A novel angiotensin-converting enzyme-related carboxypeptidase (ACE2) converts angiotensin I to angiotensin-(1–9). *Circ Res* 2000; 87: 1–9.
9. Shah A, Gul R, Yuan K, et al. Angiotensin-(1–7) stimulates high atrial pacing-induced ANP secretion via Mas/PI3-kinase/Akt axis and Na⁺/H⁺ exchanger. *Am J Physiol Heart Circ Physiol* 2010; 298: 1365–1374.
10. Zhao J, Liu E, Li G, et al. Effects of the angiotensin-(1–7)/Mas/PI3K/Akt/nitric oxide axis and the possible role of atrial natriuretic peptide in an acute atrial tachycardia canine model. *J Renin Angiotensin Aldosterone Syst* 2015; 16: 1069–1077.
11. Yue L, Feng J, Li GR, et al. Transient outward and delayed rectifier currents in canine atrium: Properties and role of isolation methods. *Am J Physiol* 1996; 270 (6 Pt 2): H2157–H2168.
12. Li D, Melnyk P, Feng J, et al. Effects of experimental heart failure on atrial cellular and ionic electrophysiology. *Circulation* 2000; 101: 2631–2638.
13. Archacki SR, Angheloiu G, Tian XL, et al. Identification of new genes differentially expressed in coronary artery disease by expression profiling. *Physiol Genomics* 2003; 15: 65–74.
14. You SA, Archacki SR, Angheloiu G, et al. Proteomic approach to coronary atherosclerosis shows ferritin light chain as a significant marker: Evidence consistent with iron hypothesis in atherosclerosis. *Physiol Genomics* 2003; 13: 25–30.
15. Försti I, Bara AT, Busse R, et al. Release of nitric oxide by angiotensin-(1–7) from porcine coronary endothelium: Implications for a novel angiotensin receptor. *Br J Pharmacol* 1994; 111: 652–654.
16. Iwata M, Cowling RT, Gurantz D, et al. Angiotensin-(1–7) binds to specific receptors on cardiac fibroblasts to initiate antifibrotic and antitrophic effects. *Am J Physiol Heart Circ Physiol* 2005; 289: 2356–2363.
17. Yoshida T, Niwano S, Niwano H, et al. Atrial natriuretic peptide (ANP) suppresses acute atrial electrical remodeling in the canine rapid atrial stimulation model. *Int J Cardiol* 2008; 123: 147–154.
18. Nattel S and Li D. Ionic remodeling in the heart: Pathophysiological significance and new therapeutic opportunities for atrial fibrillation. *Circ Res* 2000; 87: 440–447.
19. Nakashima H and Kumagai K. Reverse-remodeling effects of angiotensin II type 1 receptor blocker in a canine atrial fibrillation model. *Circ J* 2007; 71: 1977–1982.
20. Liu E, Xu Z, Li J, et al. Enalapril, irbesartan, and angiotensin-(1–7) prevent atrial tachycardia-induced ionic remodeling. *Int J Cardiol* 2011; 146: 364–370.
21. Yue L, Melnyk P, Gaspo R, et al. Molecular mechanisms underlying ionic remodeling in a dog model of atrial fibrillation. *Circ Res* 1999; 84: 776–784.
22. Gaspo R, Sun H, Fareh S, et al. Dihydropyridine and beta adrenergic receptor binding in dogs with tachycardia-induced atrial fibrillation. *Cardiovasc Res* 1999; 42: 434–442.
23. Tan AY and Zimetbaum P. Atrial fibrillation and atrial fibrosis. *J Cardiovasc Pharmacol* 2011; 57: 625–629.
24. Burstein B and Nattel S. Atrial fibrosis: Mechanisms and clinical relevance in atrial fibrillation. *J Am Coll Cardiol* 2008; 51: 802–809.
25. Rosenberg MA, Das S, Pinzon PQ, et al. A novel transgenic mouse model of cardiac hypertrophy and atrial fibrillation. *J Atr Fibrillation* 2012; 2: 1–15.
26. Platonov PG, Mitrofanova LB, Orshanskaya V, et al. Structural abnormalities in atrial walls are associated with presence and persistency of atrial fibrillation but not with age. *J Am Coll Cardiol* 2011; 58: 2225–2232.
27. Wu CH, Hu YF, Chou CY, et al. Transforming growth factor- β 1 level and outcome after catheter ablation for nonparoxysmal atrial fibrillation. *Heart Rhythm* 2013; 10: 10–15.
28. Lin X, Wu N, Shi Y, et al. Association between transforming growth factor β ₁ and atrial fibrillation in essential hypertensive patients. *Clin Exp Hypertens* 2015; 37: 82–87.
29. Canpolat U, Oto A, Hazirolan T, et al. A prospective DE-MRI study evaluating the role of TGF- β ₁ in left atrial fibrosis and implications for outcomes of cryoballoon-based catheter ablation: New insights into primary fibrotic atriacardiomyopathy. *J Cardiovasc Electrophysiol* 2015; 26: 251–259.
30. Cao H, Xue L, Wu Y, et al. Natriuretic peptides and right atrial fibrosis in patients with paroxysmal versus persistent atrial fibrillation. *Peptides* 2010; 31: 1531–1539.
31. Govindan M, Borgulya G, Kiotsekoglou A, et al. Prognostic value of left atrial expansion index and exercise-induced change in atrial natriuretic peptide as long-term predictors of atrial fibrillation recurrence. *Europace* 2012; 14: 1302–1310.

32. Edwards BS, Zimmerman RS, Schwab TR, et al. Atrial stretch, not pressure, is the principal determinant controlling the acute release of atrial natriuretic factor. *Circ Res* 1988; 62: 191–195.
33. Yoon YE, Kim HJ, Kim SA, et al. Left atrial mechanical function and stiffness in patients with paroxysmal atrial fibrillation. *J Cardiovasc Ultrasound* 2012; 20: 140–145.
34. Santos RA, Castro CH, Gava E, et al. Impairment of in vitro and in vivo heart function in angiotensin-(1–7) receptor MAS knockout mice. *Hypertension* 2006; 47: 996–1002.
35. Dias-Peixoto MF, Santos RA, Gomes ER, et al. Molecular mechanisms involved in the angiotensin-(1–7)/Mas signaling pathway in cardiomyocytes. *Hypertension* 2008; 52: 542–548.
36. Miao L, Wang M, Yin WX, et al. Atrial natriuretic peptide regulates Ca^{2+} channel in early developmental cardiomyocytes. *PloS One* 2010; 5: e8847.
37. Fujita S, Shimojo N, Terasaki F, et al. Atrial natriuretic peptide exerts protective action against angiotensin II-induced cardiac remodeling by attenuating inflammation via endothelin-1/endothelin receptor A cascade. *Heart Vessels* 2013; 28: 646–657.
38. Miura SI, Nakayama A, Tomita S, et al. Comparison of aldosterone synthesis in adrenal cells, effect of various AT1 receptor blockers with or without atrial natriuretic peptide. *Clin Exp Hypertens* 2015; 37: 353–357.
39. Moubarak M, Magaud C, Saliba Y, et al. Effects of atrial natriuretic peptide on rat ventricular fibroblasts during differentiation into myofibroblasts. *Physiol Res* 2015; 64: 495–503.
40. Oliver PM, Fox JE, Kim R, et al. Hypertension, cardiac hypertrophy, and sudden death in mice lacking natriuretic peptide receptor A. *Proc Natl Acad Sci U S A* 1997; 94: 14730–14735.